Conference Proceedings of the Society for Experimental Mechanics Series

Amalia Martínez-García · Cosme Furlong
Bernardino Barrientos · Ryszard J. Pryputniewicz *Editors*

Emerging Challenges for Experimental Mechanics in Energy and Environmental Applications, Proceedings of the 5th International Symposium on Experimental Mechanics and 9th Symposium on Optics in Industry (ISEM-SOI), 2015

Springer

Conference Proceedings of the Society for Experimental Mechanics Series

Series Editor

Kristin B. Zimmerman, Ph.D.
Society for Experimental Mechanics
Bethel, CT, USA

More information about this series at http://www.springer.com/series/8922

Amalia Martínez-García • Cosme Furlong • Bernardino Barrientos
Ryszard J. Pryputniewicz
Editors

Emerging Challenges for Experimental Mechanics in Energy and Environmental Applications, Proceedings of the 5th International Symposium on Experimental Mechanics and 9th Symposium on Optics in Industry (ISEM-SOI), 2015

Springer

Editors
Amalia Martínez-García
Senior Researcher
Centro de Investigaciones en Óptica
Leon, Mexico

Cosme Furlong
Mechanical Engineering Department
Worcester Polytechnic Institute
Worcester, MA, USA

Bernardino Barrientos
Senior Researcher
Centro de Investigaciones en Óptica
Leon, Mexico

Ryszard J. Pryputniewicz
Science and Technology (NEST)
Worcester Polytechnic Institute
Worcester, MA, USA

ISSN 2191-5644 ISSN 2191-5652 (electronic)
Conference Proceedings of the Society for Experimental Mechanics Series
ISBN 978-3-319-28511-5 ISBN 978-3-319-28513-9 (eBook)
DOI 10.1007/978-3-319-28513-9

Library of Congress Control Number: 2016940959

Printed on acid-free paper

This Springer imprint is published by Springer Nature
The registered company is Springer International Publishing AG Switzerland

Preface

This volume contains a series of technical papers presented at the Fifth International Symposium on Experimental Mechanics and Ninth Symposium on Optics in Industry (ISEM-SOI2015) organized by the Society for Experimental Mechanics (SEM), Academia Mexicana de Óptica, and Centro de Investigaciones en Óptica (CIO) and held in Guanajuato, Guanajuato, Mexico, August 17–21, 2015.

Symposia were dedicated as part of the celebrations of the International Year of Light 2015 and the XXXV anniversary of the founding of the CIO and having a general topic relating to the emerging challenges for experimental mechanics in energy and environmental applications.

This collection of papers presents early findings of experimental and computational investigations on important areas of Experimental Mechanics. Symposia were intended to be interdisciplinary forums for engineers, technicians, researchers, and managers involved in all fields of Optics, Opto-mechatronics, Mechanics, and Mechanical Engineering. Overall, papers were assigned to the following relevant tracks:

Non-destructive methods
Dynamic and static structure and substructure testing
Multi-scale fields
Advanced new materials and their characterization
Environmental measuring techniques

The organizers thank the authors, presenters, and session chairs for their participation, support, and contribution to these Symposia.

Leon, Mexico — Amalia Martínez-García
Worcester, MA — Cosme Furlong
Leon, Mexico — Bernardino Barrientos
Worcester, MA — Ryszard J. Pryputniewicz

Contents

1 **Optical Imaging Through Horizontal-Path Turbulence: A New Solution to a Difficult Problem** 1
William T. Rhodes, Nishantha Randunu Pathirannehelage, Diego Pava, and Yezid Torres Moreno

2 **Aluminum Strain Measurement by Beam Propagation** 7
Alonso Saldaña Heredia, Pedro A. Márquez Aguilar, and Arturo Molina Ocampo

3 **The Technique of Laser-Induced Breakdown Spectroscopy for Determination of Heavy Metals in the Receiving Body of Water** 19
A. Frías, A.E. Villarreal, F.G. Rendón Sauz, T. Flores, L. Ponce, R. Ortega, and M. Domínguez

4 **Applications of Laser Induced Breakdown Spectroscopy in the Identification of Bacteria** 29
F.G. Rendón Sauz, T. Flores Reyes, R. Ortega Izaguirre, A.K. Frias, A.E. Villarreal, and L. Ponce

5 **Residual Stresses Measurement by the Hole-Drilling Technique and DSPI Using the Integral Method with Displacement Coefficients** 35
Armando Albertazzi Jr, Filipe Zanini, Matias Viotti, and Celso Veiga

6 **On the Separation of Complete Triaxial Strain/Stress Profiles from Diffraction Experiments** 43
H. Wern

7 **Quantification of Slow Mechanical Displacements in Metal Samples by Optical Polarization Phase Shift DSPI** 49
Darwin Mayorga Cruz, José Antonio Marbán Salgado, Víctor Manuel Juárez Núñez, and Álvaro Zamudio Lara

8 **Comparative Analysis of Optoelectronic Properties of Glucose for Non-invasive Monitoring** 55
Jesús García-Guzmán, Naara González-Viveros, and Héctor H. Cerecedo-Núñez

9 **Phase Shifting Interferometry Using a Coupled Cyclic Path Interferometers** 65
L. García Lechuga, N.I. Toto-Arellano, V.H. Flores Muñoz, Amalia Martínez-García, and G. Rodríguez Zurita

10 **Identification of Microorganisms Using Digital Holographic Microscopy** 71
S. Muñoz Solís, M. del Socorro Hernández-Montes, and F. Mendoza Santoyo

11 **Noise Reduction in Off-Axis Digital Holography Reconstruction from Two Reconstruction Distances Based on Talbot Effect** 75
Miguel León-Rodríguez, Raúl R. Cordero, Juan A. Rayas, Amalia Martínez-García, Adrián Martínez-Gonzalez, Fernando Labbe, and Victor Flores-Muñoz

12 **Study of Temperature Distribution Over a Stirling Engine by Using the Schlieren Technique** 85
C. Alvarez-Herrera, A.R. Moreno-Nieto, and J.G. Murillo-Ramírez

13 **On Axis Fringe Projection** 93
Analía Sicardi-Segade, J.C. Estrada, Amalia Martínez-García, and Guillermo Garnica

14 Instrument for Recording Purkinje Images 101
I.U. Cosme-Cisneros, G.A. Escamilla-Ruiz, D. Flores-Montoya, G. Hernández-Gómez, and A. Gómez-Vieyra

15 Ultrasonic Arc Maps and Its Potential Application in Non-destructive Testing 111
Fabio Tomás Moreno Ortiz, Antonio Hernández Zavala, Alejandro Gómez Hernández, and Noé Emir Rodríguez Olivares

16 Phase-Shifting Generated by Wavelength Modulation by Means of Switching On-Off a Laser Diode 117
Uriel Rivera-Ortega and Joris Dirckx

17 Index of Refraction Measurements in Liquid Substances of Full Field Using Holographic Interferometry 123
Carlos Guerrero-Mendez, Tonatiuh Saucedo-Anaya, M. Araiza-Esquivel, Enrique De la Rosa, and Carlos Olvera-Olvera

18 Geometrical Thickness Measurement of Thin Films by a Transmitted Gaussian Beam 131
Moisés Cywiak, Octavio Olvera-R, and Joel Cervantes-L

19 Topography and Color Study of an Object Using Fringe Projection and Colorimetry Techniques 135
Y. Yanet López D., Amalia Martínez-García, and Julián Gómez S.

20 Temperature Measurement of a Synthetic Jet Produced by a Helmholtz Cavity 145
Alan D. Blanco M., Bernardino Barrientos G., Andrew J. Moore, and Carlos Mares C.

21 Gates' Interferometer as Fringe Projection System for Recovering 3D Shapes 153
J.A. Rayas, M. León-Rodríguez, Amalia Martínez-García, and R.R. Cordero

22 Development of an Automated Laser Induced Breakdown Spectroscopy System for Compositional Mapping of Surfaces 159
E. Ponce Flores, J.R. Domínguez Torres, R. Galindo Del Valle, and A.E. Villarreal

23 Artificial Visual System Used for Dental Fluorosis Discrimination 165
Miguel Mora-González, Evelia Martínez-Cano, Francisco J. Casillas-Rodríguez, Francisco G. Peña-Lecona, Carlos A. Reyes-García, Jesús Muñoz-Maciel, and H. Ulises Rodríguez-Marmolejo

24 Inspection of Laser Ablated Transparent Conductive Oxide Thin Films by a Multifunction Optical Measurement System 173
Chi-Hung Hwang, Ming-Hsing Shen, Shih-Feng Tseng, Wen-Tse Hsiao, I-Feng Cheng, and Wei-Chung Wang

25 LIBS Technique for Identification of Crude Oils 181
F.G. Rendón, A.K. Frías, A.E. Villarreal, T. Flores, L. Ponce, and G. Vázquez-Bautista

26 3D Displacement Distribution Measurement Using Sampling Moire Method with Multiple Cameras 187
Daiki Tomita, Yorinobu Murata, and Motoharu Fujigaki

27 Automatic Generation of Codes for Routine of CNC Machining Based on Three-Dimensional Information Obtained by Fringe Projection 195
S. Bustos, C. Aguilera, and Amalia Martínez-García

28 Automatic Generation of Movement Sequences to Robotic Arm Based on Three-Dimensional Data Obtained Through Fringe Projection Technique 203
S. Bustos, C. Aguilera, and Amalia Martínez-García

29 Application of Optomecatronics Load Cell for Measuring Work Force and Efforts in Industrial Machinery 211
A.A. Camacho and F.J. Martínez-Serrano

30 ASE Noise Attenuation for Signal at 1548.4 nm Through a Sagnac Interferometer Using High-Birefringence Fiber Which Is Subjected to Temperature Changes 215
Manuel May-Alarcón, Héctor H. Cerecedo-Núñez, Aarón Flores-Gil, Miguel A. García-González, Francisco Méndez-Martínez, Marco A. Rodríguez-Blanco, and Víctor Golikov

31 Single-Shot Phase Shifting Interferometry for Microscopic Measurements of Non-Birefringent Transmissive Phase Samples 221
V.H. Flores Muñoz, B. López Ortiz, N.I. Toto-Arellano, Amalia Martínez-García, and G. Rodríguez Zurita

32 Design of a Customized Myoelectric Hand Prosthesis 227
A.A. Silva-Moreno and E. Lucas Torres

33 Finite Element Static Analysis Simulation for a Grain Dispenser Mechanism 233
J.E. Valtierra, A.A. Silva, B.L. Vargas, and E.A. Ruelas

34 Controlling Bounce of Vacuum Circuit Breakers' Contacts 241
Masao Narita, Naoki Yaegashi, Minoru Kobayashi, and Shigeru Inaba

35 Experimental and Numerical Investigation of Effects of Fiber Orientation of Wood Stiffness 249
Tzu-Yu Kuo and Wei-Chung Wang

36 Auto-Calibration and Micro-Flow Injection Procedure Based on Automated Hydrodynamic System for Spectrophotometric Determination of Cobalt 255
R.M. Camarillo E., J.A. Padilla M., J.A. García M., C.A. Ocón D., Ch. Reyes C., J.M. Camarillo E., and R. Rodríguez R.

37 Mathematical Model to Predict the Stress Concentration Factor on a Notched Flat Bar in Axial Tension 265
F.J. Ortega-Herrera, A. Lozano-Luna, J.P. Razón-González, J.M. García-Guzmán, and F. Figueroa-Godoy

38 Mechanical Implementation of Kinematic Synergy for Multi-Point Grasping 273
M.A. Trejo Letechipia, J.A. Cortes Ramírez, and H. Aguayo Téllez

39 Cascaded Ultra-Low Reflective Fiber Points for Distributed Sensing 281
Rodolfo Martinez Manuel and H.E. Sutherland

40 Object Surface Representation Via NURBS and Genetic Algorithms with SBX 289
J. Apolinar Muñoz Rodríguez and Francisco Calos Mejia Alanís

41 Photo-Oxidation of Polystyrene Film Irradiated with UV-B 295
C.G. Hernández, R. González, J.J. Soto, and I. Rosales

42 Dynamic Analysis of Trawl Doors Applied in Bottom Trawls to Catch Shrimp 301
S. Sarmiento-Nafaté, J. Enríquez-Zárate, J. Villalobos-Toledo, and C. Pineda-García

43 Simulator of an Adaptive Optics System Using Matlab 311
Marco A. Betanzos-Torres, Juan Castillo-Mixcóatl, Severino Muñoz-Aguirre, and Georgina Beltrán-Pérez

44 Design, Development and Validation of an Artificial Muscle Biomechanical Rig (AMBR) for Finite Element Model Validation 319
A. Kriechbaumer, M.P. Trejo Ramírez, U. Mittag, M. Itskov, J.M. López Ramírez, and J. Rittweger

45 Application of Laser Light on the Development of Equipment for the Study of Proteins 329
Nydia Tejeda Muñoz and Martha Robles-Flores

46 Organic Solar Photovoltaic Cells 335
A. Nava-Vega, Mario Cerda Lemus, Denisse Makoske Ibarra, and Moisés Viloria Sánchez

47 Fiber Bragg Gires-Tournois Interferometer Etalons as Fiber Sensor 341
A. González-García, C.I. Castañeda-Jiménez, N. Rico-Jordan, I. Urbina-Salas, G. González-García, and M.C. Wilson-Herrán

48 Cleaning of Tantalum Capacitor Electrode Surface by Laser in Multipulse Regime 345
A.E. Villarreal, A.K. Frías, F.G. Rendón, T. Flores, L. Ponce, and G. Vázquez-Bautista

49 High Quality Polishing Procedure of Glass Substrates: Application in Integrated Optics 355
H.E. Lazcano, J.L. Flores, A. Blanco, A. Hernández, R. Nieto, J.L. Martínez, R.A. Torres, G.V. Vázquez, and J.L. Hurtado

Index 365

Chapter 17
Index of Refraction Measurements in Liquid Substances of Full Field Using Holographic Interferometry

Carlos Guerrero-Mendez, Tonatiuh Saucedo-Anaya, M. Araiza-Esquivel, Enrique De la Rosa, and Carlos Olvera-Olvera

Abstract We present a novel method based on Digital Holographic Interferometry to detect slight physical variations of refractive index with high sensitivity in liquid substances. The technique is grounded in the measurement of a phase difference between two reconstructed wavefields. The optical system was tested using a series of sodium chloride (NaCl) solutions to detect a variation in its physical property such as concentration. A first hologram records a wavefront coming from the light scattered by a common cylindrical glass container filled with certain NaCl solution. Later, a second hologram is recorded when the solution mentioned above slightly changes its concentration. The difference between the phase maps obtained from the correlation from the two holograms will provide information about a refractive index variation, which is directly related to a concentration change. The achieved results have proven to be more accurate and faster to get than with other techniques. The process requires just a few special optical elements and is able to measure the three-dimensional distribution of the refractive index of a sample. This method can be extended to identify adulteration in liquids, measure the variation in refractive index in gaseous flames, apart from analyzing and visualizing the mechanical properties of a liquid sample.

Keywords Digital holographic interferometry • Phase measurement • Refractive index • Phase difference • Non-destructive methods

17.1 Introduction

Physical properties of liquids such as concentration, weight, color and others are important parameters that can be used as an identification tool or "fingerprint" of some solutions [1, 2]. Likewise analysis of the variations of one or more of such parameters is important to some areas of science. For example, in medicine, the study of certain physiological fluids (like urine) is an important aspect that may indicate the state of health of the body [3]. Generally speaking, detailed analysis of any variations in parameters in a medical solution can mark the difference for a suitable treatment of a disease when necessary [4]. On the other hand, adulteration problems in many commercial substances have increased in the last days, and we require reliable and simple techniques to detect changes of the liquid properties that can help controlling adulteration of liquids [5].

Optical techniques are able to detect changes in concentration of liquid solutions through measurements of the unique optical parameter of a medium called refractive index [6, 7]. The typical optical technique to determine a refractive index utilizes the displacement of the angle of a beam refracted by a sample, and these methods use a prism [8–11], square [12, 13] and special containers [14]. Additionally, these methods are easy to implement and understand, and require few optical elements. However the refracted angle is difficult to measure, and ultimately you can only make a good estimation of the measured angle, which decreases the accuracy of measurements and we can only get the refractive index in the illuminated region [15].

Advanced optical techniques of full-field, non-destructive, non-contact, non-invasive nature with a metrology potential to detect a variety of physical parameters variation in fluids with high resolution and stability have been developed [16–18]. These are called Schlieren, Shadowgraph, Interferometry techniques, from which DHI arised [19].

C. Guerrero-Mendez (✉) • M. Araiza-Esquivel • E. De la Rosa • C. Olvera-Olvera
Doctorado en Ciencias de la Ingeniería, Facultad de Ingeniería Eléctrica, Universidad Autónoma de Zacatecas, Av. Ramón López Velarde #801, Zacatecas C.P. 98000, Mexico
e-mail: capacti@gmail.com

T. Saucedo-Anaya
Unidad Académica de Física, Universidad Autónoma de Zacatecas, Calzada Solidaridad Esq. Con Paseo La Bufa S/N, Zacatecas C.P. 98060, Mexico

A. Martínez-García et al. (eds.), *Emerging Challenges for Experimental Mechanics in Energy and Environmental Applications, Proceedings of the 5th International Symposium on Experimental Mechanics and 9th Symposium on Optics in Industry (ISEM-SOI), 2015*, Conference Proceedings of the Society for Experimental Mechanics Series, DOI 10.1007/978-3-319-28513-9_17

Important works have established methods to measure the refractive index values using DHI [20], which may be related with the concentration of the liquid solution [21, 22]. However, these researches consider the thickness of the container as known.

In this work we present a simple, fast, full-field, non-destructive, high-precision technique to measure the refractive index of a liquid solution. The method can detect slight differences in concentration of liquid mixtures, through the relationship between concentration and refractive index. The method detects differences on the order of ±0.007 % with the thickness of the mixture container unknown. The system was tested using sodium chloride solutions. The obtained results show consistence with data published in [23].

17.2 Principles and Experimental Setup

The experimental setup is shown in Fig. 17.1. A monochromatic light coming from He-Ne laser with a wavelength $\lambda = 543\,\text{nm}$ and a maximum output power of 15 mW is divided into two beams by a Beam splitter BS1. The transmitted beam (called "an object beam") impinges on a mirror M1 and is reflected towards the lenses L1, L2 and the diffuser D1, in such a way that it illuminates the common glass tube that contains the liquid sample S to be analyzed. Part of the light enters through a rectangular aperture A1 and is collected by a positive lens L3 that forms the image of the tube with the sample in the Charge-Coupled Device (CCD) sensor. The reflected beam (named "the reference beam") travels through a single mode optical fiber SSMF1, and is sent into the cube beam splitter BS2 placed in front of the CCD in such a manner that it interferes with the "object beam" in the CCD sensor. As an initial step, a hologram (H1) is recorded coming from the first mixture sample (named s_1). The CCD is a mono color sensor with 1280 × 1024 pixels (1.3 MP). During the experiment the temperature was controlled at 20 °C. The wavefront scattered by the glass tube in this first state can be represented as a complex amplitude as $U_1(x,y) = u_1(x,y)\exp[i\varphi_1(x,y)]$, with $u_1(x, y)$ the real amplitude and $\varphi_1(x, y)$ the phase.

A second hologram (H2) is recorded when the solution in the tube is slightly modified in its concentration (creating the sample s_2). This second state or mixture in the glass is represented as $U_2(x,y) = u_2(x,y)\exp[i(\varphi_1(x,y) + \Delta\varphi(x,y))]$ or simply $U_2(x,y) = u_2(x,y)\exp[i\varphi_2(x,y)]$. The phase map from each hologram is calculated using the method of the Fourier-transform [24, 25]. Figure 17.2a shows the hologram of the common glass tube filled with a sample liquid. Fig. 17.2b shows one example of the Fourier-transform of an intensity distribution recorded with the arrangement shown in Fig. 17.1. We can filter out the central term and one of the images of the aperture and keep the other as shown in Fig. 17.2c.

The phase of a wavefront is related to the optical path length δ via $\varphi = 2\pi\delta/\lambda$. This path length is linked with the morphology and physical properties of the transmitting medium as $\delta = nd$, where n is the index refraction and d as the thickness of the sample. According to cylinder geometry, the phase of a hologram can be described as:

$$\varphi = k\left[(d_t - d_i)^* n_g + d_i^* n_s\right],$$

where $k = 2\pi/\lambda$; d_i and d_t are the inner and outer diameters of the glass tube respectively; n_s and n_g are the known refractive indices of the mixture and the glass respectively. See Fig. 17.3.

To get a quantity value of the refractive index difference between any two liquid samples, called s_1 and s_2, we use their phase terms to calculate a phase difference $\left(\Delta\varphi_{s_2-s_1} = \varphi_{s_2} - \varphi_{s_1}\right)$ and generate a phase map described as:

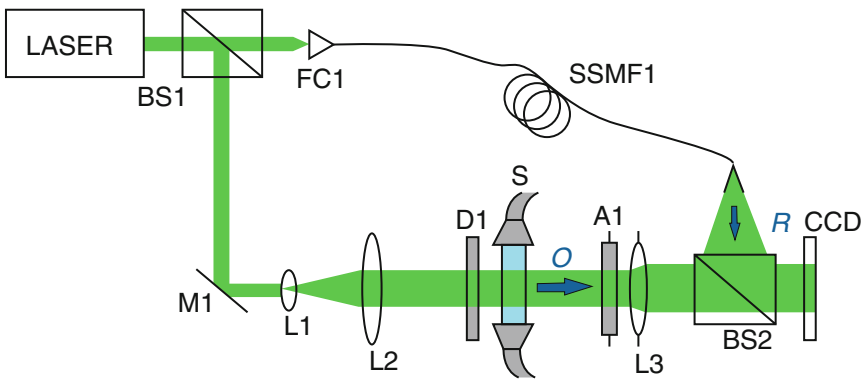

Fig. 17.1 Experimental setup using the DHI. *BS1, BS2* cube beam splitters, *FC1* fiber collimator, *M1* mirror, *L1, L2, L3* lenses, *SSMF1* single mode fiber, *S* sample liquid (glass tube), *D1* diffuser, *A1* aperture, *O* object beam, *R* reference beam

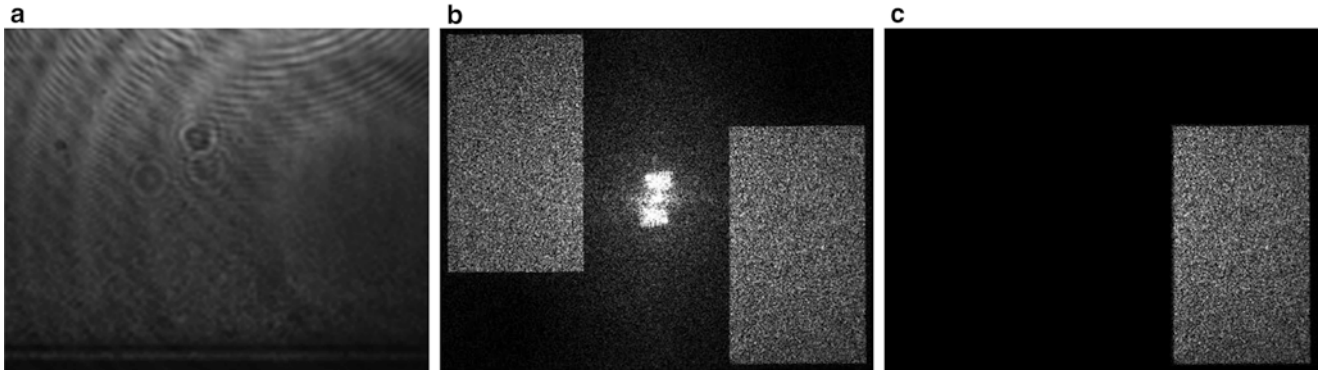

Fig. 17.2 A Fourier-transform method. (**a**) Digital hologram of the container; (**b**) separated Fourier spectra with the image of the aperture; and (**c**) single spectrum selected

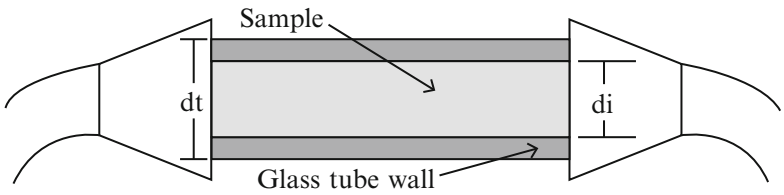

Fig. 17.3 Shows the glass tube with the liquid sample. d_i inner diameter, d_t outer diameter

$$\Delta\varphi_{s_2-s_1} = kd_i(n_{s_2} - n_{s_1}), \tag{17.1}$$

Using (17.1) we can calculate a refractive index difference between aqueous substances, but given that in our optical system, the phase object or the tube used is an ordinary glass cylinder whose walls are optically imperfect and thickness measurements are unknown (d_i). To solve this, we use a liquid with known properties values; this can be a reference solution s_o to create an expression that eliminates the dependence on this parameter. We construct

$$d_i = \frac{\Delta\varphi_r}{\Delta n_r} k^{-1}, \tag{17.2}$$

where $\Delta\varphi_r = \varphi_{s_1} - \varphi_{s_0}$ is the phase difference obtained (called "of reference") from the two known liquid substances and Δn_r is the index refraction difference of them.

Using (17.1) and (17.2) we can get the value of the refractive index difference between two substances as:

$$\Delta n_{2-1} = \frac{\Delta n_r}{\Delta\varphi_r}\Delta\varphi_{2-1}, \tag{17.3}$$

To get a refractive index value regarding our reference value, (17.3) changes as:

$$n_{s_2} = \frac{\Delta n_r}{\Delta\varphi_r}\Delta\varphi_{2-0} + n_{s_o}, \tag{17.4}$$

where $\Delta\varphi_{2-0} = \Delta\varphi_{2-1} + \Delta\varphi_{1-0}$.

17.3 Experimental Method and Results

In order to calculate and visualize an index refraction distribution in a liquid sample, we use three liquid substances, two of them have known values of index refraction and molarity (s_1 and s_0), and the last substance has a refractive index unknown (s_2). The optical system was tested using a series of solutions with a certain amount of sodium chloride (NaCl) to be

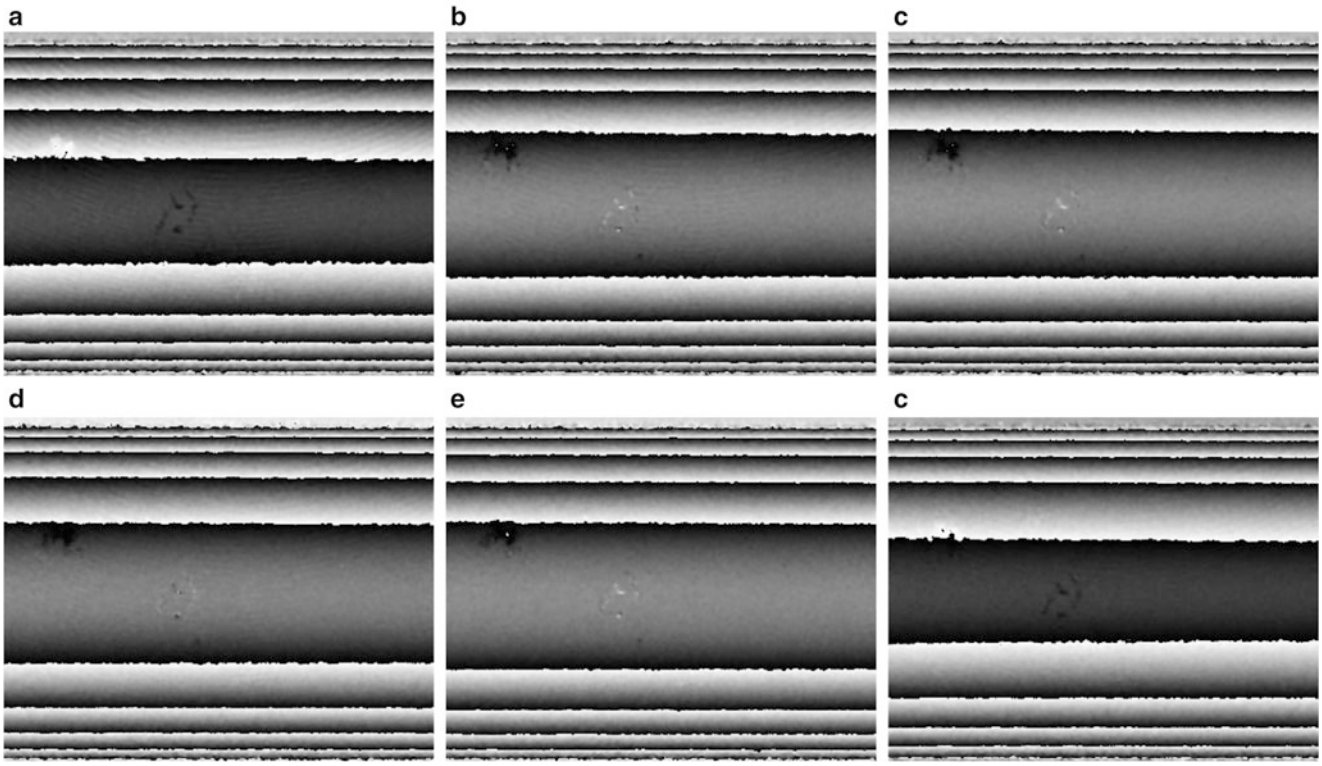

Fig.17.4 Maps of wrapped phase difference. Samples: (**a**) $s_2 = 0.086$ mol and $s_1 =$ distilled water, (**b**) $s_2 = 0.172$ mol and $s_1 = 0.086$ mol, (**c**) $s_2 = 0.258$ mol and $s_1 = 0.172$ mol, (**d**) $s_2 = 0.344$ mol and $s_1 = 0.258$ mol, (**e**) $s_2 = 0.43$ mol and $s_1 = 0.344$ mol, (**f**) $s_2 = 0.516$ mol and $s_1 = 0.43$ mol

compared with the values found in [23]. A first hologram with the tube filled with distilled water is recorded and was used as s_0 in all our experiments. After that, a series of holograms are recorded with their corresponding saline solution (with 0.086, 0.172, 0.258, 0.344, 0.430, 0.516 mol). The phase reference was created using distilled water (s_0) and the solution with 0.086 mol (s_1). Then a series of phase difference maps are obtained from the correlation between the holograms calculated from the solution that works as the unknown liquid sample (i.e. s_2) and the next substance with a lower concentration (s_1). See Fig. 17.4.

The n_{s_0} value in (17.4) is the known value determined for the distilled water $(n_{s_0} = 1.3330)$. If we use the n_{s_0} and the value from the correlation between solutions (i.e. in $\Delta\varphi_{2-0}$), it is very high and produces a wrapped phase map that has high frequencies (see Fig. 17.5). We will have to add more small values in (17.4). The small parts are unwrapped (see Fig. 17.6), in such a way that allows us to calculate the refractive index of s_2.

Table 17.1 shows the deviation in the refractive indices measured by the method proposed and those found in [23] that are approximately ± 0.007 %.

The method proposed using the DHI allows to visualize the distribution of the refractive index value of full-field and is linked with the different physical properties in the liquid sample. See Fig. 17.7. Figure 17.8 shows the comparison of the values obtained among those found in [23].

17.4 Conclusions

In this paper, we report a new method to detect with a high sensibility a possible variation on the physical properties of a liquid by the DHI. The process registers phase variations between wavefields scattered by full-field liquid samples. The method is inexpensive, noninvasive, fast and easy to develop in a laboratory. The technique can resolve extremely small changes in refractive index, on the order of 0.007 %, that is, differences of ± 0.0001 of accuracy in comparison to the value of the refractive index reported in [23]. In addition to this, the method does not use a special device to hold the aqueous sample and neither is it necessary to know the inner diameter d_i and n_g, that refer to the thickness and the refractive index of

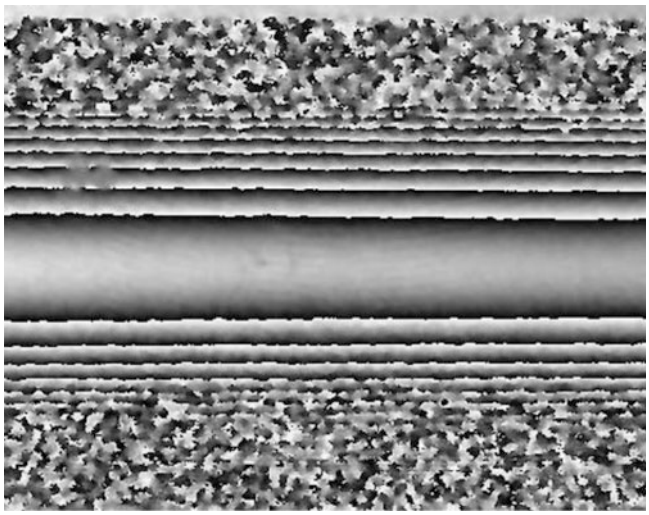

Fig. 17.5 Wrapped phase map that has high frequencies ($s_2 = 0.516$ mol and $s_0 =$ distilled water)

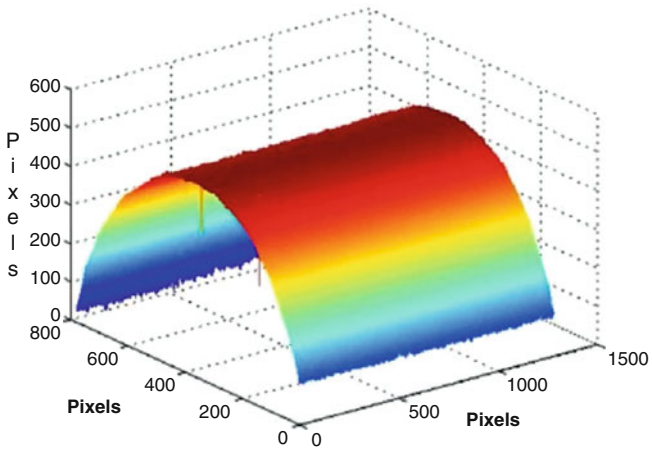

Fig. 17.6 Phase unwrapped ($s_2 = 0.0866$ mol and $s_1 =$ distilled water)

Table 17.1 Comparisons among refractive indices measured by the DHI and those found in [23]

Molarity	Index refraction in [23]	Index refraction (n_{s_2}) measured with DHI
0.086	1.3339	1.3339
0.172	1.3347	1.3348
0.258	1.3356	1.3357
0.344	1.3364	1.3365
0.430	1.3373	1.3374
0.516	1.3382	1.3383

the glass tube respectively, and are considered negligible values for another similar researches. The method can be extended to study a variety of applications requiring noncontact, real-time remote monitoring of liquid concentration and to identify liquid adulterations.

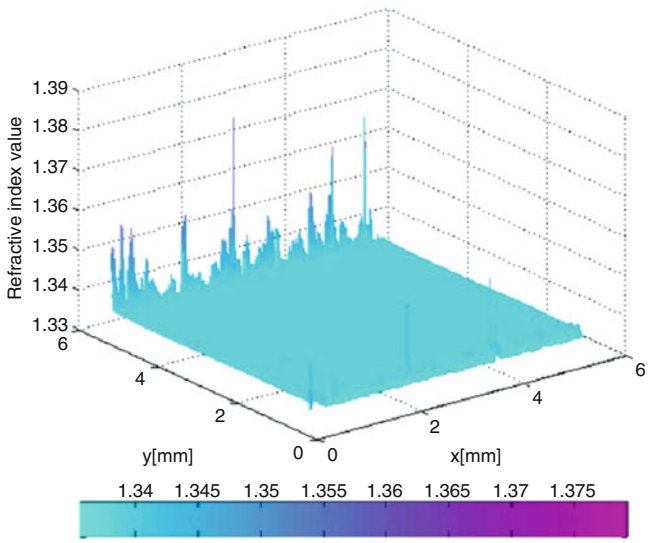

Fig. 17.7 Full-field index refraction distribution on the liquid sample with 0.516 mol

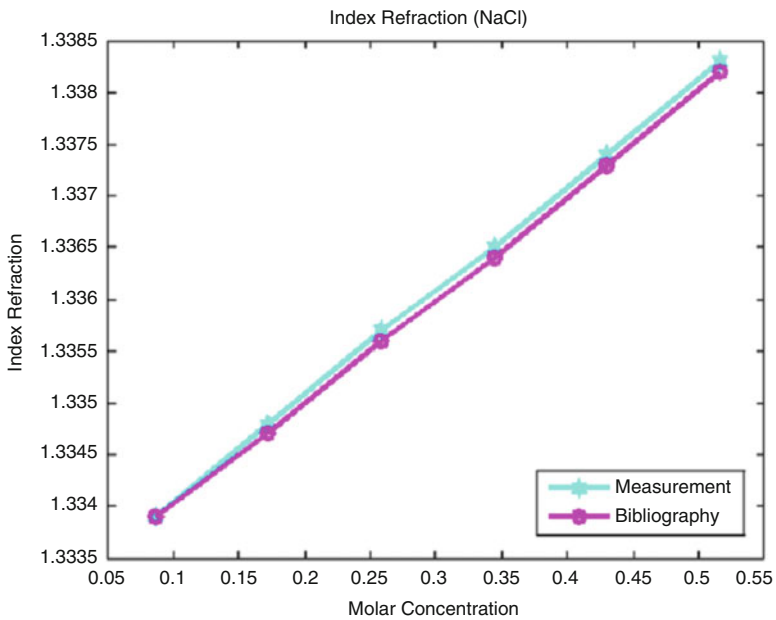

Fig. 17.8 Shows refractive indices calculated and those found in [23]

Acknowledgments The authors acknowledge Prof. S. Guel Sandoval for the useful suggestions and encouraging comments, for the suggestions on this paper. On the other hand, one of the authors (Carlos Guerrero-Mendez) acknowledges CONACYT (Mexico) for providing partial financial support for this work, and the helpful assistance of Sonia A. Saucedo for the technical support.

References

1. M. Cracolice, *Basics of Introductory Chemistry with Math Review* (Brooks/Cole, Belmont, 2006)
2. J.W. Moore, C.L. Stanitski, P.C. Jurs, *Principles of Chemistry: The Molecular Science* (Cengage Learning, Belmont, 2009)
3. R.W. Schrier, *Diseases of the Kidney and Urinary Tract*, vol. 1 (Lippincott Williams & Wilkins, Philadelphia, 2007)
4. A. Smit, A. O'Byrne, *Introduction to Bioregulatory Medicine* (Thieme, Stuttgart, 2011)
5. C.K. Kokate, A.P. Purohit, S.B. Gokhale, *Pharmacognosy*, 42nd edn. (Nirali Prakashan, Pune, 2006)
6. M. Satake, Y. Hayashi, Y. Mido, S.A. Iqbal, M.S. Sethi, *Colloidal and Surface Chemistry* (Discovery Publishing House, New Delhi, 2003)
7. G.V. Karas, *New Topics in Crystal Growth Research* (Nova, New York, 2006)

8. B.P. Chandra, S.C. Bhaiya, A simple, accurate alternative to the minimum deviation method of determining the refractive index of liquids. Am. J. Phys. **51**(160), 160–161 (1983)
9. B.W. Grange, W.H. Stevenson, R. Viskanta, Refractive index of liquid solutions at low temperatures: an accurate measurement. Appl. Opt. **15**(4), 858–859 (1976)
10. M.D. Edmiston, Measuring refractive indices. Phys. Teach. **24**(260), 160–163 (1986)
11. M.R. Shenoy, S. Roy, K. Thyagarajan, Simple prism coupling technique to measure the refractive index of a liquid and its variation with temperature. Rev. Sci. Instrum. **61**(3), 1010–1013 (1990)
12. J.P. Longtin, C.-H. Fan, Precision laser-based concentration and refractive index measurement of liquids. Microscale Thermophys. Eng. **2**, 261–272 (1998)
13. S. Nemoto, Measurement of the refractive index of liquid using laser beam displacement. Appl. Opt. **31**(31), 6690–6694 (1992)
14. E. Moreels, C. de Greef, R. Finsy, Laser light refractometer. Appl. Opt. **23**(17), 3010–3013 (1984)
15. S. Singh, Refractive index measurements and its applications. Phys. Scr. **65**, 167–180 (2002)
16. C.M. Vest, *Holographic Interferometry* (Wiley, New York, 1979)
17. J. Colombani, J. Bert, Holographic interferometry for the study of liquids. J. Mol. Liq. **134**, 8–14 (2007)
18. T. Kreis, *Handbook of Holographic Interferometry: Optical and Digital Methods* (Wiley, Weinheim, 2005)
19. R. Goldstein, *Fluid Mechanics Measurements* (CRC Press, New York, 1996)
20. M.M. Hossain, D.S. Mehta, C. Shakher, Refractive index determination: an application of lensless fourier digital holography. Opt. Eng. **45**(10), 1062031–1062037 (2006)
21. Y. Zhang, J. Zhao, J. Di, H. Jiang, Q. Wang, J. Wang, Y. Guo, D. Yin, Real-time monitoring of the solution concentration variation during the crystallization process of protein-lysozyme by using digital holographic interferometry. Opt. Express **20**, 18415–18421 (2012)
22. J. Zhao, Y. Zhang, H. Jiang, J. Di, Dynamic measurement for the solution concentration variation using digital holographic interferometry and discussion for the measuring accuracy, in *International Conference on Optics in Precision Engineering and Nanotechnology Proc. of SPIE*, vol. **8769**, 2013, pp. 87690D1–87690D18
23. W. Haynes, *Concentrative Properties of Aqueous Solutions: Density, Refractive Index, Freezing Point Depression, and Viscosity CRC Handbook of Chemistry and Physics*, 92nd edn. (CRC Press, Boca Raton, 2012)
24. M. Takeda, H. Ina, S. Kobayashi, Fourier-transform method of fringe-pattern analysis for computer-based topography and interferometry. J. Opt. Soc. Am. **72**(1), 156–160 (1982)
25. A.T. Saucedo, F. Mendoza Santoyo, M. De la Torre-Ibarra, G. Pedrini, W. Osten, Endoscopic pulsed digital holography for 3D measurements. Opt. Express **14**, 1468–1475 (2006)